UTAH GEOLOGICAL SURVEY
a division of
Utah Department of Natural Resources

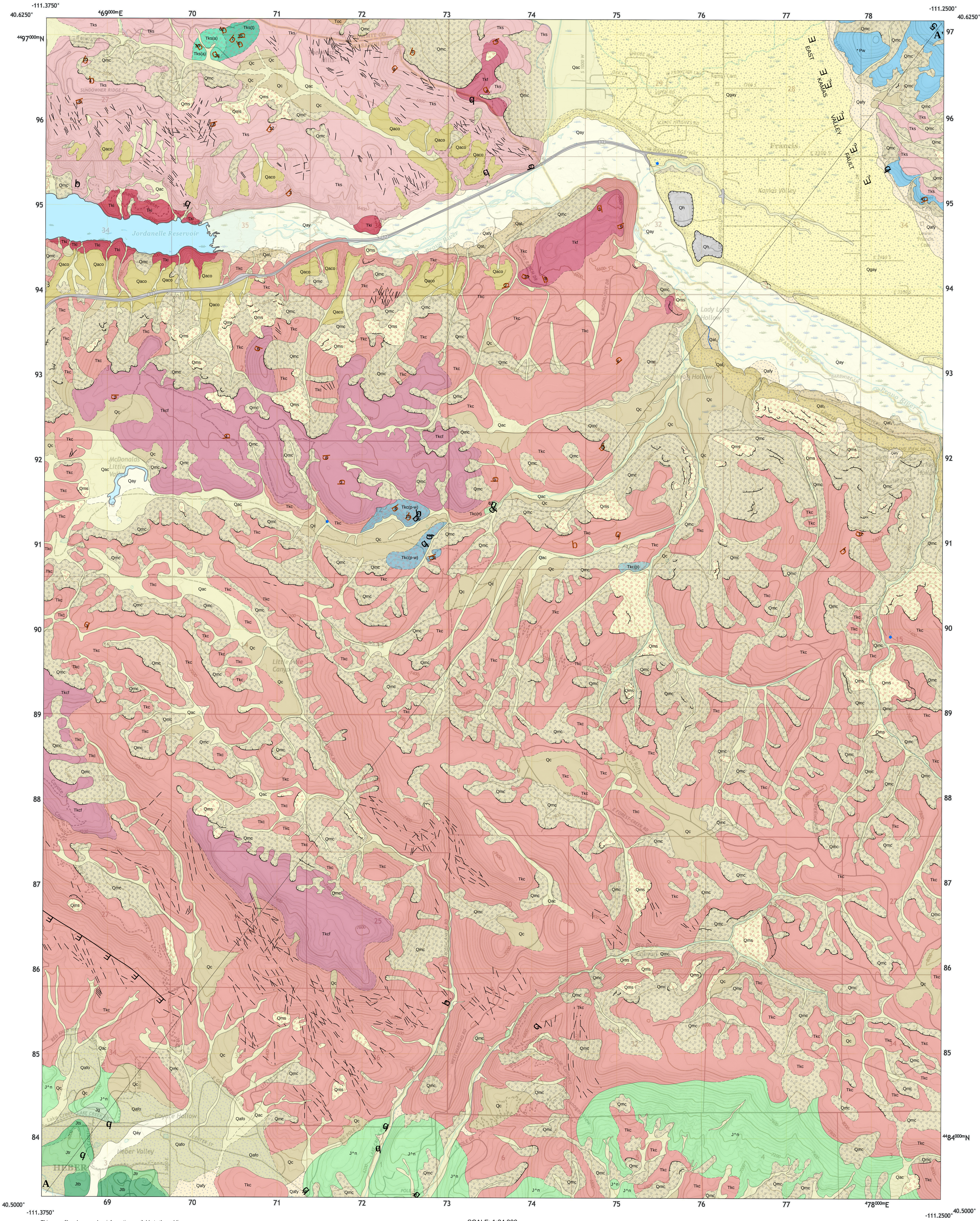

This open-file release makes information available to the public that has undergone only minimal peer review and may not conform to Utah Geological Survey technical, editorial, or policy standards. The map may be incomplete, and inconsistencies, errors, and omissions have not been resolved. The Utah Department of Natural Resources, Utah Geological Survey, makes no warranty, expressed or implied, regarding the suitability of this product for a particular use, and does not guarantee accuracy or completeness of the data. The Utah Department of Natural Resources, Utah Geological Survey, shall not be liable under any circumstances for any direct, indirect, special, incidental, or consequential damages with respect to claims by users of this product. For use at 1:24,000 scale.

This geologic map was funded by the Utah Geological Survey and the U.S. Geological Survey, National Cooperative Geologic Mapping Program, through USGS STATEMAP award number G23AC00466 (2023–2025). The views and conclusions contained in this document are those of the author and should not be interpreted as necessarily representing the official policies, either expressed or implied, of the U.S. Government.

SCALE: 1:24,000

1 0.5 0 1 MILE

1000 0 1000 2000 3000 4000 5000 6000 7000 FEET

1 0.5 0 1 KILOMETER

CONTOUR INTERVAL 40 FEET

10°34′ TRUE NORTH MAGNETIC NORTH

APPROXIMATE MEAN DECLINATION, 2025

UTAH

MAP LOCATION

INTERIM GEOLOGIC MAP OF THE FRANCIS QUADRANGLE, SUMMIT AND WASATCH COUNTIES, UTAH

by

Lauren J. Reeher[1] and Abigail E. Conger[2]

2025

[1]Utah Geological Survey, Salt Lake City, Utah
[2] Utah Valley University, Department of Earth Science, Orem, Utah

Base from USGS US Topo Francis 7.5′ Quadrangle (2023)
Shaded relief derived from USGS 10-meter NED
Projection: UTM Zone 12
Datum: NAD 1983

Program Manager: Stefan M. Kirby
Project Manager: Matthew C. Morriss
GIS and Cartography: Subigya Shah
Geology Review: Matthew C. Morriss and Stefan M. Kirby
GIS and Cartography Review: Josh A. Dustin and Austin J. Jensen

Utah Geological Survey
1594 West North Temple, Suite 3110
Salt Lake City, UT 84116
(801) 537-3300
https://geology.utah.gov

https://doi.org/10.34191/OFR-770DM

1	2	3
4		5
6	7	8

1. Park City East
2. Kamas
3. Hoyt Peak
4. Heber City
5. Woodland
6. Charleston
7. Center Creek
8. Heber Mountain

ADJOINING 7.5′ QUADRANGLE NAMES

MAP UNITS

see booklet for complete unit descriptions

QUATERNARY-PLIOCENE (TERTIARY)

- Qh — Artificial fill and disturbed land
- Qay — Younger stream alluvium and floodplain deposits
- Qafy — Younger alluvial-fan deposits
- Qafo — Older alluvial-fan deposits
- Qat_1 — Stream terrace deposits
- Qat_2 — Stream terrace deposits
- Qgay — Younger glacial outwash
- Qc — Colluvial deposits
- Qms — Landslide deposits
- Qac — Alluvial and colluvial deposits, undivided
- Qaco — Older alluvial and colluvial deposits
- Qmc — Mass-movement and colluvial deposits, undivided

PALEOGENE (TERTIARY)

- Tki — Provo River intrusive rocks
- Tkf — Lava flows of Francis Quarry
- Tkcf — Lava flows of Coyote Canyon
- Tkc — Volcanic mudflow breccia of Coyote Canyon
- Tkc(n) — Coyote Canyon chaos, Nugget Sandstone
- Tkc(p) — Coyote Canyon chaos, Park City Formation
- Tkc(p-w) — Coyote Canyon chaos, Park City Formation and Weber Sandstone
- Tks — Volcanic mudflow breccia of Silver Creek
- Tks(a) — Silver Creek chaos, Ankareh Formation, undivided
- Tks(t) — Silver Creek chaos, Thaynes Formation, undivided
- Toc — Older conglomerate

JURASSIC

- Jtb — Twin Creek Limestone, Boundary Ridge Member
- Jtr — Twin Creek Limestone, Rich Member
- Jts — Twin Creek Limestone, Slide Rock Member
- Jg — Gypsum Spring Formation

JURASSIC-TRIASSIC

- JŦn — Nugget Sandstone

TRIASSIC

- Ŧa — Ankareh Formation, undivided
- Ŧt — Thaynes Formation
- Ŧw — Woodside Shale

shown on cross section only

PERMIAN-PENNSYLVANIAN

- Pp — Park City and Phosphoria Formations, undivided — *shown on cross section only*
- IPPw — Weber Sandstone

PENNSYLVANIAN-DEVONIAN

- IPDu — Pennsylvanian through Devonian rocks, undivided — *shown on cross section only*

CAMBRIAN-NEOPROTEROZOIC

- ЄZu — Cambrian through Neoproterozoic rocks, undivided — *shown on cross section only*

CORRELATION OF MAP UNITS

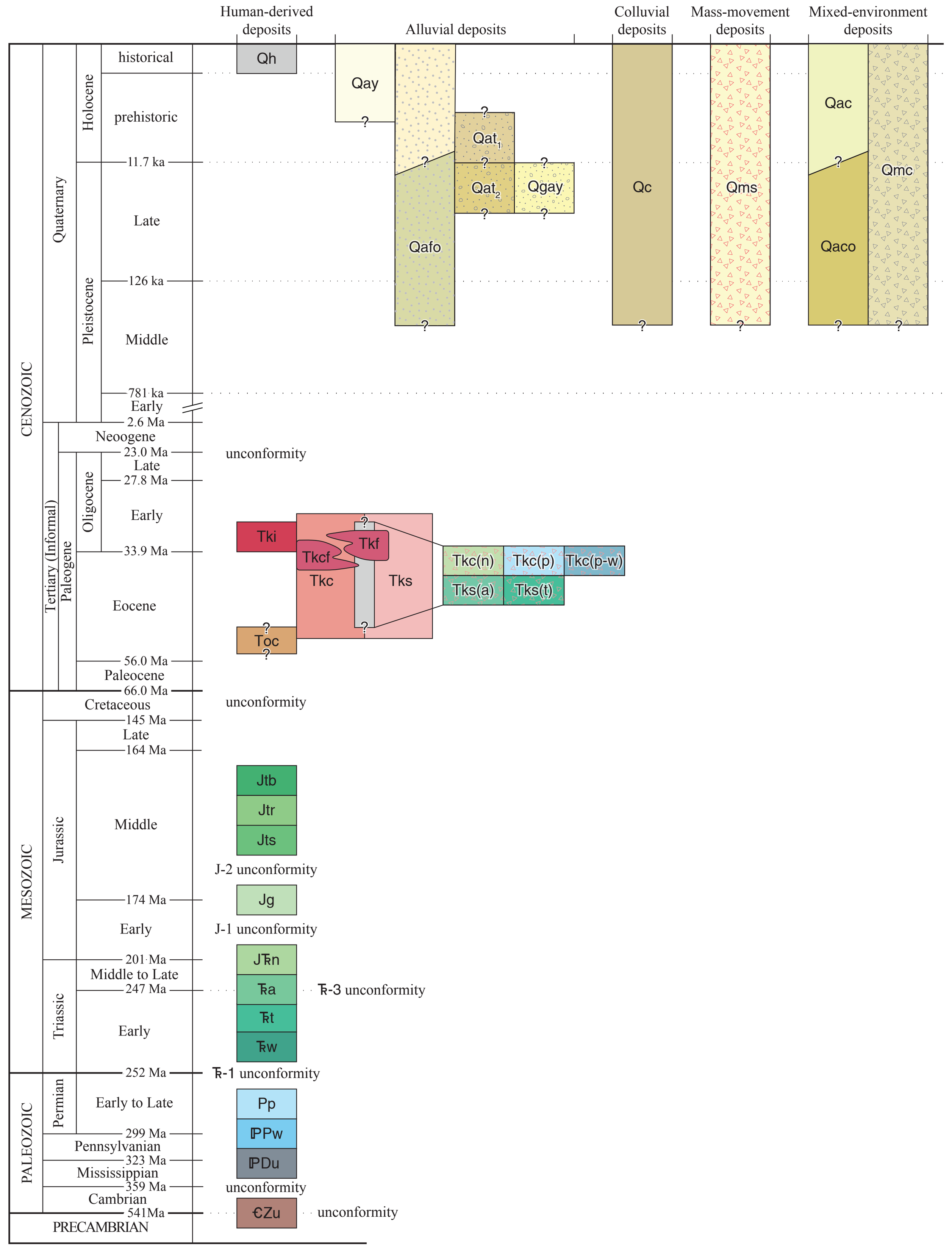

SELECTED SOURCES OF GEOLOGIC MAPPING

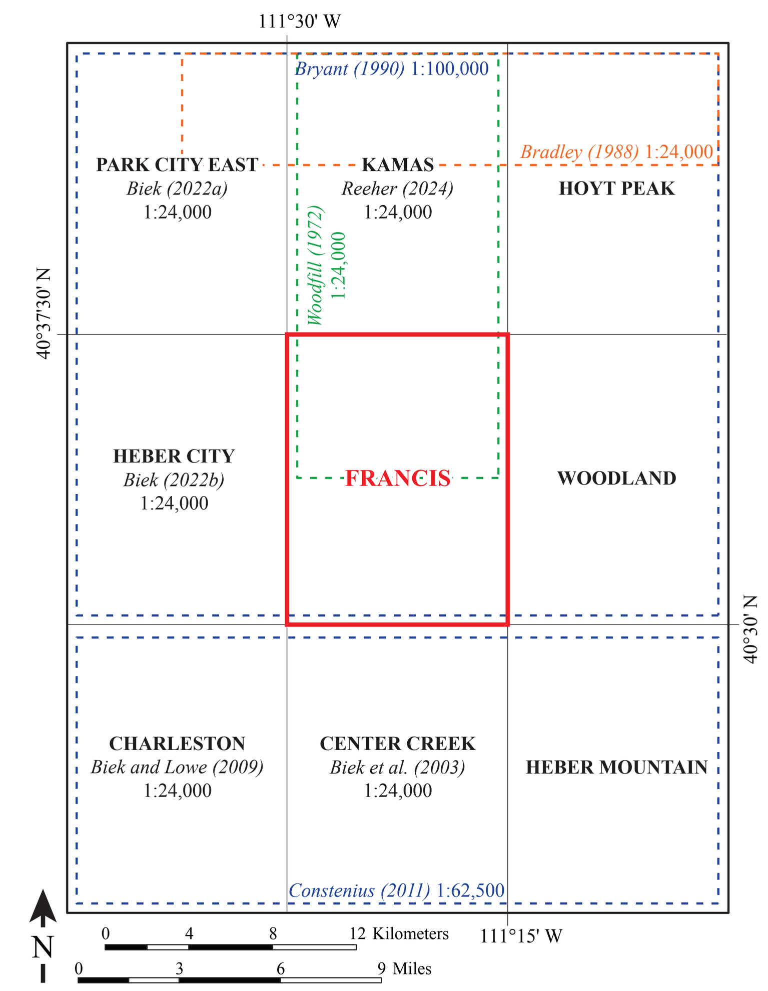

GEOLOGIC SYMBOLS

- Contact – Dashed where approximately located, hashed where gradational, dotted where concealed
- Normal fault – Dashed where approximately located, dotted where concealed, queried where existance uncertain, ball and bar on downthrown side; arrows on cross section indicate direction of relative movement
- Landslide scarp – ticks on downdropped side
- Lineament; visible on aerial photography and lidar; likely consists of joint zones
- A——A′ Line of cross section
- Outline of aggregate sand and gravel pit operations
- Erosional terrace in Qat_1 – ticks point downhill
- 65 65 Strike and dip of inclined bedding – red symbols indicate attitudes form Woodfill (1972)
- 65 Strike and dip of inclined bedding extracted from lidar in *findSD* software (Conners et al., 2023)
- Spring

LITHOLOGIC COLUMN

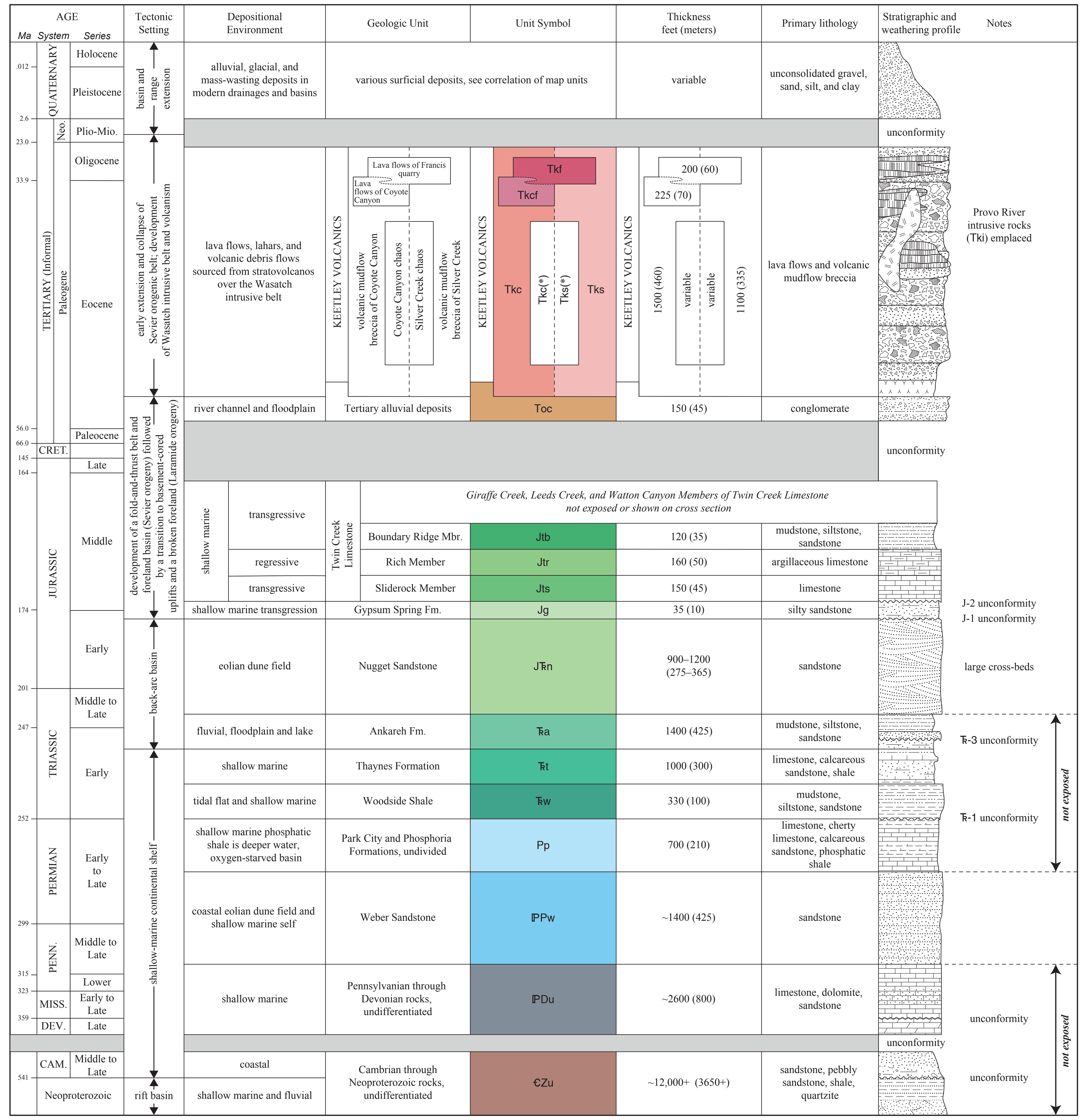

unit may not be exposed or exposed thickness may not be complete in map area. See unit descriptions for more information.

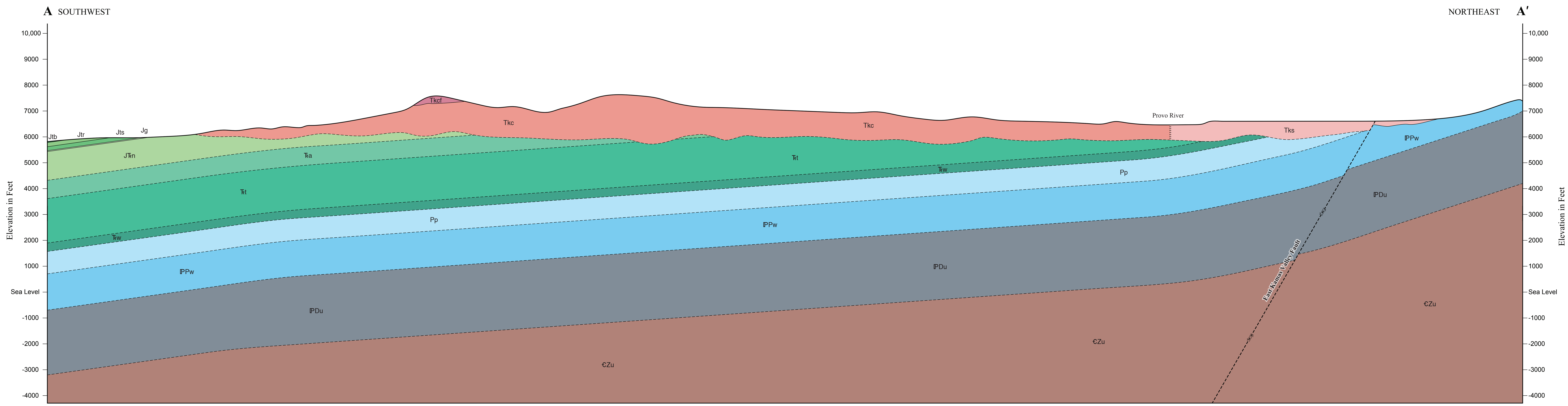

thin superficial units not shown

INTERIM GEOLOGIC MAP OF THE FRANCIS QUADRANGLE, SUMMIT AND WASATCH COUNTIES, UTAH

by

Lauren J. Reeher[1] and Abigail E. Conger[2]

[1]Utah Geological Survey, Salt Lake City, Utah
[2]Utah Valley University, Department of Earth Science, Orem, Utah

Suggested citation:

Reeher, L.J. and Conger, A.E., 2025, Interim geologic map of the Francis quadrangle, Summit and Wasatch Counties, Utah: Utah Geological Survey Open-File Report 770DM, 15 p., 2 plates, scale 1:24,000, https://doi.org/10.34191/OFR-770DM.

This geologic map was funded by the Utah Geological Survey and the U.S. Geological Survey, National Cooperative Geologic Mapping Program, through USGS STATEMAP award number G23AC00466 (2023–2025). The views and conclusions contained in this document are those of the author and should not be interpreted as necessarily representing the official policies, either expressed or implied, of the U.S. Government.

UTAH DNR GEOLOGICAL SURVEY

OPEN-FILE REPORT 770DM
UTAH GEOLOGICAL SURVEY
UTAH DEPARTMENT OF NATURAL RESOURCES
2025

Blank pages are intentional for printing purposes.

INTRODUCTION

Location and Geography

The Francis quadrangle (Plate 1) is in Summit and Wasatch Counties of the Wasatch Back in Northern Utah, approximately 30 miles (50 km) southeast of Salt Lake City, Utah. Elevation ranges from 5900 feet (1800 m) to 8100 feet (2500 m) above sea level. It includes the town of Francis, the eastern part of Jordanelle Reservoir and Jordanelle State Park, the northeastern margin of Heber Valley, and the southern extent of Kamas Valley. The Provo River flows westward, from the southwestern Uinta Mountains, through the northern part of the quadrangle and into Jordanelle Reservoir. The Francis quadrangle lies within the Middle Rocky Mountains physiographic province (Fennemen and Johnson, 1946) and is bordered by the Wasatch Range to the west and the Uinta Mountains to the northeast.

Geologic Overview

Along the northern margin of the Uinta Mountains a Neoproterozoic (~770 to 740 Ma) suture zone, known as the Cheyenne Belt, marks the northern boundary of a faulted rift basin that accumulated up to 23,000 feet (7000 m) of Uinta Mountain Group sediments, which consists of gravel, sand, and mud (Bryant and Nichols, 1988; Houston et al., 1993). These Neoproterozoic rocks are exposed in the Uinta Mountains 3 miles (5 km) east of the Francis quadrangle (Bryant, 1990). The Proterozoic rift basin was later inverted through episodic uplift during Phanerozoic time, resulting in the east-west-trending Uinta arch, with the most recent Laramide uplift event occurring from Late Cretaceous to Paleogene (Crittenden, 1976; Bruhn et al., 1986; Yonkee et al., 2014). The Uinta arch is part of the large Uinta-Tooele structural zone that extends across the length of the Uinta Mountains and continues westward through the Cottonwood Canyons of the Wasatch Range to Tooele, Utah (Clark et al., 2020). The Uinta-Tooele structural zone (Clark, 2020) is marked by a suture in the Precambrian basement, a zone of Tertiary igneous rocks that extend west from the Francis quadrangle, and localized uplifts during Phanerozoic time (Yonkee et al., 2014; Clark et al., 2020). Kamas Valley forms a structural low between the Uinta and Cottonwood arch segments of the Uinta-Tooele structural zone. The Uinta arch segment plunges west beneath the valley, whereas the Cottonwood arch segment plunges east beneath the valley. This structural saddle is obscured by a blanket of Paleogene volcanic rocks and Neogene basin fill (Bradley and Bruhn, 1988; Bryant and Nichols, 1988).

Perpendicular to the Uinta and Cottonwood arches, the Cordilleran hinge line demarcates a dramatic westward thickening of late Proterozoic to Paleozoic sediments (Picha and Gibson, 1985; Hintze, 1988). The Cordilleran hinge line formed during late Proterozoic rifting of the North American continent, with subsequent Paleozoic strata deposited along a long-lived passive margin. The Great Unconformity in the Uinta Mountains region separates the Neoproterozoic Uinta Mountain Group from overlying Phanerozoic strata beginning with the basal Cambrian Tintic Quartzite (Eardley and Hatch, 1940; Peters and Gaines, 2012). The Tintic Quartzite is absent in the Francis region due to uplift and erosion during Silurian to Middle Devonian time along the Uinta arch (Bruhn et al., 1986; Bryant and Nichols, 1988). Upper Devonian to Pennsylvanian strata (~2600 feet [800 m] thick), mostly marine carbonates deposited in a stable shelf environment, are the oldest preserved Paleozoic rocks in the region and are exposed within 1 mile (1.6 km) northeast of the Francis quadrangle. The Pennsylvanian-Permian Weber Sandstone is the oldest bedrock exposed in the quadrangle, near the northeastern boundary, and has a stratigraphic thickness of about 1400 feet (425 m). Pennsylvanian to Permian rocks (Weber Sandstone and Park City Formation) consist of limestone and sandstone deposited in shallow marine and coastal environments. The Park City Formation is obscured by Paleogene volcanic rocks in the quadrangle, but estimates based on nearby exposures suggest a thickness of 850 feet (260 m) in the region.

Early Mesozoic rocks in the region reflect a transition from primarily shallow marine and nearshore deposition to terrestrial deposystems, with episodic marine incursions (Thomas and Krueger, 1946). Although the Triassic section (Woodside Shale, Thaynes Formation, and Ankareh Formation) is covered by Paleogene volcanic rocks in the Francis quadrangle, exposures in neighboring quadrangles are primarily composed of reddish mudstone, shale, siltstone, sandstone, and limestone with a combined thickness of about 2730 feet (825 m) (Bryant, 1990). The overlying Jurassic/Triassic Nugget Sandstone was deposited as a coastal eolian dune field that extended across much of the western United States (Kocurek and Dott, 1983; Blakey, 1994; Peterson, 1994). In the Francis region, the Nugget Sandstone ranges from 900 to 1200 feet (275–365 m) thick. A Middle Jurassic transgression of the Sundance Seaway submerged the Nugget dunes, and deposition of the Middle Jurassic Twin Creek Limestone followed in a warm, shallow inland sea (Imlay, 1967, 1980). An incomplete section of the Twin Creek Limestone is the youngest non-volcanic rock, exposed near the southeastern boundary of the quadrangle.

This stratigraphic section was later deformed and uplifted by Cordilleran tectonism related to Sevier and Laramide deformation. The Sevier fold-and-thrust belt, active from Jurassic to Paleogene time, was related to eastward subduction of the Farallon plate beneath North America (Allmendinger, 1992; DeCelles, 1994; Yonkee and Weil, 2015). Sevier-style deformation, characterized by thin-skinned thrust faults, developed a fold-and-thrust belt to the west and north of the Francis quadrangle (Bryant, 1990), along with an associated foreland basin. This north-south-trending foreland basin formed east of the Cordilleran fold-and-thrust belt during Cretaceous to Early Eocene time, where fluvial and marine sediments derived from erosion of rocks uplifted by thrusts and folds accumulated (Royse et al., 1975; Lamerson, 1982; Royse, 1993; DeCelles, 1994). The Cordilleran foreland basin was later broken by a series of thick-skinned basement-cored uplifts and intervening basins formed during Laramide deformation (Dickinson and Snyder, 1978; Bird, 1984; Bruhn et al., 1986; Bradley, 1995; Yonkee and Weil, 2015; Weil and Yonkee, 2023). These two orogenic styles overlap in time and space in the vicinity of the Francis quadrangle (Yonkee and Weil, 2015).

Laramide deformation is distinct from Sevier-style thin-skinned deformation and characterized by broad reverse-fault-bounded basement-cored uplifts and intervening basins. The Laramide Uinta arch is a major, doubly plunging, east-west basement-cored anticlinal structure formed by shortening along reverse faults on its northern (North Flank fault) and southern (South Flank fault) margins (Bruhn et al., 1986; Sullivan et al., 1988). Flexural subsidence adjacent to the Uinta Laramide uplift created substantial depositional basins: the Green River Basin to the north, and the Uinta Basin to the south (Dickinson et al., 1988). Due to the extensive cover of Paleogene volcanic rocks in the Francis quadrangle, exposures of pre-volcanic bedrock are limited. Still, the southern limb of the west-plunging Uinta arch is recognizable by Paleozoic and Mesozoic strata that dip southwest, with dip magnitudes decreasing southward toward Heber Valley. Laramide deformation and uplift were followed by heightened Paleogene volcanic activity along the Uinta-Tooele structural zone.

The Francis quadrangle contains expansive exposures of the Paleogene Keetley Volcanic field. These rocks consist of andesitic to dacitic lava flows, volcaniclastic deposits, and tuffs. Intermediate composition dikes and shallow intrusions fed a series of stratovolcanoes across the Keetley Volcanic field, blanketing older rocks and preexisting structures across the Wasatch Back (Woodfill, 1972). The volcanic strata exhibit significant thickness variations, likely influenced by paleotopography at the time of deposition (Forrester, 1937; O'Toole, 1951; Woodfill, 1972; Feher, 1997) and maximum thickness ranges from about 1100 feet (335 m) to 1500 feet (460 m) in the quadrangle. Woodfill (1972) defined an internal stratigraphy for the Keetley Volcanics, which is maintained in this and adjoining maps (Biek, 2022a; Biek, 2022b; Reeher, 2024). This stratigraphy is dominated by volcanic mudflow breccia with lava flow deposits and commonly exhibits a basal tuffaceous unit with complex interlayering and lateral discontinuity of layers within each volcanic unit.

Paleogene volcanism has significantly influenced the Francis region. The Indian Hollow stock and associated dike swarms, located in the Kamas quadrangle to the north, represent the easternmost extent of the Wasatch intrusive belt and are interpreted as one potential source of the Keetley Volcanic field (Bromfield, 1968; Woodfill, 1972; John, 1989a; Leveinen, 1994; Hanson, 1995; Feher, 1997; Reeher, 2024). Cross-cutting relationships suggest the Indian Hollow stock intruded through and post-dates some Keetley volcaniclastic strata (Reeher, 2024). The east-west-trending Wasatch intrusive belt includes several high-potassium, calc-alkaline Paleogene intrusions (John, 1987, 1989b; Hanson, 1995; Feher, 1997; Vogel et al., 1998; Vogel et al., 2001). The Wasatch intrusive belt stocks were emplaced between 25 and 42 Ma (see Table 2 of Biek [2022a] and references therein; Stearns et al., 2020; Jensen et al., 2022). Intrusive bodies of the Wasatch belt include, from east to west: the Indian Hollow stock, the Park Premier stock, six Park City stocks (Pine Creek, Valeo, Glencoe, Mayflower, Ontario, Flagstaff), the Clayton Peak stock, the Alta stock, and the Cottonwood stock (Bryant, 1990; Hanson, 1995). Both the silica content (Hanson, 1995) and the depth of emplacement (John, 1987, 1989b) of exposed intrusive rocks increase from east to west. Several smaller unnamed intrusive bodies are mapped near the Jordanelle Reservoir in the Francis quadrangle.

Extension and associated normal faulting related to the ongoing development of the Basin and Range Province began contemporaneously with Paleogene volcanism and has continued into the Quaternary (Zoback, 1983; Sullivan et al., 1988; Constenius, 1996). Normal faulting within the Francis region represents an eastward continuation of Basin and Range extensional faulting (Sullivan et al., 1988; Hurlow, 2002). The East Kamas Valley fault forms a half-graben system that defines the eastern boundary of Kamas Valley. Though the fault is largely concealed by Quaternary alluvial, fluvial, and mass movement deposits, its presence is indicated by gravity, well, and geomorphic data (Baker and Peterson, 1970; Sullivan et al., 1988; Hurlow, 2002). This fault is interpreted to terminate in the northeastern corner of the Francis quadrangle. The East Kamas Valley fault does not cut alluvial deposits associated with Bull Lake glaciation (130–140 Ma) (Sullivan et al., 1988) but is suggested to have early Quaternary displacement based on range front morphology and soil development (Sullivan et al., 1988; Black and Hecker, 1999).

The Francis quadrangle contains six main types of unconsolidated Quaternary deposits that include landslide deposits, colluvium, alluvium, alluvial-terrace deposits, alluvial-fan deposits, and glacial outwash deposits. Landslides are especially abundant where Keetley volcaniclastic lithologies (Tks, Tkc) are present. Colluvium covers large portions of bedrock exposures and is mapped where it is thick enough to obscure identification of the underlying bedrock. Alluvial deposits in the quadrangle are associated with the Provo River and various tributaries in the north near Kamas Valley and near Lake Creek and Center Creek to the south near Heber Valley.

The western Uinta Mountains contain abundant glacial till and outwash (Munroe and Laabs, 2009, 2017) that formed during at least three glacial episodes: Pre-Bull Lake, Bull Lake, and Pinedale (Sullivan et al., 1988; Pierce et al., 2018; Quirk et al., 2020). In Kamas Valley, a glacial outwash deposit is preserved north of the modern Provo River. Correlating the outwash deposit to specific glacial episodes is challenging due to the absence of quantitative age control and a lack of direct correlation to age-constrained glacial deposits upstream.

The modern Provo River flows west from the southwest Uinta Mountains to Utah Lake. During the Early Pleistocene, the Provo River flowed north as the south fork of the Weber River, joining the Weber River near Peoa (Anderson, 1915). Evidence of the northern flow direction is seen in the northern ridge geometry of the glacial outwash deposit (Qgay) north of the Provo River. Sullivan et al. (1988) suggest the Provo River was captured and diverted to its current course around the time of the Bull Lake glaciation (~130–140 Ma). Surface-water diversions, irrigation return flows, and an indistinct groundwater divide link the modern Weber River and Provo River drainages in Kamas Valley (Hurlow, 2002).

Previous Mapping and Methods

The geologic map of the Francis 7.5′ quadrangle provides insights into the area's geologic history and valuable information for land-use planning and hazard mitigation. This mapping effort builds upon recent adjacent 1:24,000-scale geologic mapping, including the Kamas quadrangle to the north (Reeher, 2024), the Park City East quadrangle to the northwest (Biek, 2022a), and the Heber City quadrangle to the west (Biek, 2022b). Together, these maps create a cohesive framework for understanding the region's geology and in support of planning decisions for ongoing development.

Although the southern half of the Francis quadrangle had never been mapped at 1:24,000 scale prior to this effort, the northern half was previously mapped at 1:24,000 scale by Woodfill (1972). The region has been mapped at 1:100,000 scale as part of the Salt Lake City 30′ x 60′ quadrangle by Bryant (1990). Although these maps provide a good foundation, they were used as a guide. For this new map, we have significantly expanded and improved detail of Quaternary units, improved accuracy and precision of many contacts and structures, and provided edge-matched geology (where appropriate) to recent adjoining maps by Reeher (2024) and Biek (2022b).

This interim map was prepared by the authors from 2023 to 2025, including all necessary field work. The authors compiled and mapped geology in the field and office using a combination of GPS-enabled tablets and computer-based Geographic Information Systems (GIS) equipped with georectified aerial imagery, lidar data, previously published geologic maps, topographic maps, and applications for digital attitude collection. Some mapping was done on stereographic pairs of natural color aerial photographs from the USDA National Agriculture Imagery Program (USDA NAIP, 2009). Most landslides, lineaments, and some contacts were mapped using lidar elevation data (0.5-meter data [UGRC 2020]). Line work was completed at a target scale of 1:24,000 using ESRI ArcGIS software, where the map was compiled, formatted, and completed. ArcGIS and Adobe Illustrator were used to create and compile Plate 2 materials.

DESCRIPTION OF MAP UNITS

QUATERNARY-PLIOCENE (TERTIARY)

Human-Derived Deposits

Qh **Artificial fill and disturbed land** (Historical) – Unit includes a variety of unconsolidated material in aggregate pits, engineered fill, and general borrow material used for major highways; mapped at two mining operations near Francis that extract sand and gravel from glacial outwash deposits; includes area of fill and disturbed land along Utah Highway 32; mapped where greater than 6 feet (2 m) thick.

Alluvial Deposits

Qay **Younger stream alluvium and floodplain deposits** (Holocene) – Unconsolidated sand, silt, clay, and gravel in channels, floodplains, and terraces less than 10 feet (3 m) above modern stream level; mapped along Provo River, Lake Creek, and in McDonalds Little Valley and Coyote Hollow; locally includes swamp, muddy, organic overbank and oxbow lake deposits; estimated thickness up to 40 feet (12 m).

Qafy **Younger alluvial-fan deposits** (Holocene to Late Pleistocene?) – Poorly to moderately sorted, weakly to non-stratified, clay- to boulder-size sediment primarily deposited by debris flows and debris floods at the mouths of active drainages that impinge on modern floodplains; forms characteristic lobate alluvial-fan morphology, upper parts of fans are commonly incised up to 3 feet (1 m); locally contains colluvium from adjacent slopes; thickness up to 100 feet (30 m).

Qafo **Older alluvial-fan deposits** (Late? to Middle Pleistocene?) – Poorly to moderately sorted, weakly to non-stratified, clay- to boulder-size sediment primarily deposited by debris flows and debris floods; incised up to 30 feet (10 m) by modern drainages; mapped along Lake Creek tributaries in northeastern corner of Heber Valley where unit has a discernably higher landscape position than adjoining Qafy; locally includes colluvium from adjacent slopes; estimated thickness is less than 100 feet (30 m).

Qat_1 **Stream terrace deposits** (Holocene?) – Poorly to well-sorted pebbles to boulders in a matrix of sand, silt and clay; subangular to subrounded grains and clasts; poorly to moderately bedded; exhibits erosional terrace along southern margin of Provo River floodplain; forms terraces about 30 to 70 feet (9–21 m) above the modern Provo River; typically 10 to 35 feet (3–10 m) thick.

Qat_2 **Stream terrace deposits** (Late Pleistocene?) – Poorly to well-sorted pebbles to boulders in a matrix of sand, silt and clay; subangular to subrounded grains and clasts; poorly to moderately bedded; forms terraces about 100 to 130 feet (30–40 m) above modern Provo River, similar to the position of Qgay but mapped separately due to the lack of ridge-and-swale topography and differing surface texture; typically 10 to 35 feet (3–10 m) thick.

Qgay **Younger glacial outwash** (Late Pleistocene?) – Poorly to moderately sorted, massive to moderately layered, silt- to boulder-size sediment with subrounded to rounded clasts; forms a broad, planar, gently sloping surface that displays ridge-and-swale topography likely formed by glacial outwash streams; mapped 100 to 150 feet (30–45 m) above modern Provo River flood plain; inferred as glacial outwash related to the Late Pleistocene Pinedale glaciation but age control and spatial correlation to Pinedale-age glacial deposits up drainage are lacking, hence queried age; see Munroe and Laabs (2017) for age control of the Pinedale glacial features in the Uinta Mountains and Quirk et al. (2020) in the Wasatch Range; mapped as Qgay based on its elevation above modern drainage correlating with Qgay to the north in Kamas Valley (Reeher, 2024); northward flow direction indicated by ridge-and-swale topography in Kamas Valley suggests deposition by the ancestral Provo River system that flowed north as the south fork of the Weber River (Anderson, 1915); Sullivan et al. (1988) suggested Provo River capture to its present course by headwater erosion through the West Hills of the Keetley Volcanic field around the time of Bull Lake glaciation; if true these glacial outwash deposits may be Middle Pleistocene in age; locally includes minor Holocene colluvium and alluvial deposits too small to map separately; generally less than 150 feet (45 m) thick.

Colluvial Deposits

Qc **Colluvial deposits** (Holocene to Middle Pleistocene?) – Poorly to moderately sorted, clay- to boulder-size, locally derived sediment deposited by slope wash and soil creep on moderate slopes and in shallow depressions; generally mapped in areas of gentle slopes directly below areas of steep slopes; locally includes mixed alluvial, colluvial, and talus deposits too small to map separately; much of the bedrock in the map area is covered by a thin veneer of colluvium; only mapped where deposits have significant thickness (> about 3 to 6 feet [1–2 m]) and extent; typically less than 30 feet (9 m) thick.

Mass-Movement Deposits

Qms **Landslide deposits** (Holocene to Middle Pleistocene?) – Poorly sorted, locally derived clay to boulder-size material; includes slides, slumps, and flows; characterized by hummocky topography, main and internal scarps, chaotic internal bedding in displaced blocks, and small ponds or marshy depressions; composition depends on local source; a single mapped unit may consist of multiple superimposed landslides; may exhibit slow creep or are capable of renewed movement if stability thresholds are exceeded (Ashland, 2003); age and stability determinations require detailed geotechnical investigations; many small or thin landslides may be present throughout the quadrangle but not mapped due to map scale; thickness highly variable and up to 150 feet (45 m).

Mixed-Environment Deposits

Qac **Alluvial and colluvial deposits, undivided** (Holocene to Late Pleistocene?) – Poorly to moderately sorted, poorly stratified, clay- to boulder-size locally derived sediment deposited along the sides and bottoms of secondary drainages by alluvial processes, debris flows, slope wash, and soil creep; locally reworked by ephemeral streams; locally includes mass movement deposits not differentiated due to scale; estimated thickness less than 20 feet (6 m).

Qaco **Older alluvial and colluvial deposits** (Late? to Middle Pleistocene?) – Poorly to moderately sorted, pebble to cobble gravel in a matrix of sand, silt, and clay; includes older fan, stream terrace, and colluvial deposits; mapped along tributaries north and south of the Provo River; likely contains some component of younger alluvial and colluvial deposits (Qac) from adjacent slopes and where units are indivisible due to scale; deposits have relatively smooth surfaces that grade downstream toward the Provo River; deposits may represent landscape equilibration to a northward flowing Provo River during the Pleistocene; incision increases downstream towards the main drainage to a surface that is 360 to 200 feet (110–60 m) above the Provo River; estimated thickness less than 65 feet (20 m).

Qmc **Mass-movement and colluvial deposits, undivided** (Holocene to Middle Pleistocene?) – Poorly sorted, locally derived, clay- to boulder-size material; mapped where individual landslides, slumps, slope wash, and soil creep are difficult to distinguish from one another; commonly characterized by hummocky slopes composed of numerous slumps of various sizes and ages; includes soil creep, talus, slope wash, and debris-flow deposits that may or may not have clear landslide scarps and lateral margins; typically forms on slopes of landslide-prone bedrock units such as Tks and Tkc, mapped extensively over Keetley Volcanic bedrock; estimated less than 20 feet (6 m) thick.

unconformity

PALEOGENE (TERTIARY)

Tki **Provo River intrusive rocks** (Early Oligocene) – Black to dark-grey intrusive porphyritic rock with phenocrysts of pyroxene, hornblende, and plagioclase; plagioclase and black hornblende phenocrysts (up to 2 cm long) with minor pyroxene in a microcrystalline groundmass; weathers to resistant ridges; weathered pyrite stains most of the outcrops brownish-red to whitish-yellow; flow banded; crosscutting relationship with Tkc and Tks suggest it intruded into the volcanic breccia; Woodfill (1972) suggests that this unit is partly extrusive based on field relationships; mapped along eastern extent of Jordanelle reservoir; thickness unknown.

Keetley extrusive volcanic rocks (Early Oligocene to Late Eocene) – The volcanic stratigraphy of the quadrangle consists of light-gray andesitic to dacitic lava flows, mudflow lahar deposits, fine-grained ash-fall tuffs, volcaniclastic conglomerates, and debris avalanche deposits. These diverse lithologies exhibit interfingering relationships and lateral discontinuity, indicative of a complex and dynamic depositional environment. For mapping purposes, these deposits are divided into four units: volcanic mudflow breccia of Silver Creek (Tks); volcanic mudflow breccia of Coyote Canyon (Tkc); lava flows of Francis Quarry (Tkf); and lava flows of Coyote Canyon (Tkcf). The Tks and Tkc units, both composed primarily of volcanic mudflow breccias and volcaniclastic conglomerates with interbedded lava flows and ash-fall tuffs, are likely a single depositional unit, distinguished only by their location north (Tks) and south (Tkc) of the Provo River. Numerous lineaments, likely representing joints with minor displacement related to volcanic collapse or cooling, are visible in lidar and aerial imagery within the Tks and Tkc units, often highlighted by linear vegetation patterns. These lineaments are restricted to the mudflow breccia and conglomerate units, and absent in the lava flows, possibly due to the unique geomechanical properties of the ash-rich matrix within the mudflow breccias. Dips within the volcanic units appear primary, suggesting minimal tectonic tilting, and an angular discordance is observed between the volcanic rocks and the underlying bedrock (Bromfield, 1968; Woodfill, 1972). The deposits were laid down on considerable topographic relief, resulting in significant thickness variations (Forrester, 1937; O'Toole, 1951; Woodfill, 1972; Feher, 1997). These units are eastward extensions of those mapped by Biek (2022b) in the Heber City quadrangle, and southern extensions of those mapped by Reeher (2024) in the Kamas quadrangle. The total thickness of these deposits varies considerably, exceeding 2500 feet (760 m) southeast of Heber City (Biek et al., 2003), reaching up to 1650 feet (500 m) north of Heber City (Leveinen, 1994), and attaining up to 2050 feet (625 m) within the Francis quadrangle.

Tkf **Lava flows of Francis Quarry** (Early Oligocene to Late Eocene) – Medium-grey, pyroxene-rich latite porphyry; 1–3 mm phenocrysts of white plagioclase and green pyroxene make up about 30% of the rock, the remaining 70% consists of gray aphanitic groundmass and weathered hornblende laths; outcrops west of Francis; exhibit well-developed vertical cooling joints in exposure south of the Provo River; 120 feet (35 m) thick.

Tkcf **Lava flows of Coyote Canyon** (Early Oligocene to Late Eocene) – Gray latite porphyry lava flows with 20% to 30% phenocrysts of plagioclase commonly 1 to 2 mm and as much as 5 mm in size, and less abundant and smaller phenocrysts of hornblende and biotite in a fine-grained groundmass; caps the volcanic breccia of Coyote Canyon north of Heber City; 200 to 250 feet (60–75 m) thick.

Tkc **Volcanic mudflow breccia of Coyote Canyon** (Early Oligocene to Late Eocene) – Andesitic volcanic mudflow breccia similar and likely equivalent to that of the volcanic breccia of Silver Creek (Tks); mapped south of the Provo River; light-gray andesitic to rhyodacitic volcanic mudflow deposits with minor ash-flow tuff and lava flows; clasts are andesite and rhyodacite in field but chemically range from latite and trachyte to andesite and dacite (Bromfield et al., 1977); clasts commonly 5 to 10 feet (1.5–3 m) in diameter, consisting of brecciated, weathered, and unidentifiable igneous and local sedimentary rock fragments; volcaniclastic rocks are typically heterolithic but in places are monolithic (Biek, 2022b); best exposed in road cuts at Victory Ranch south of Provo River; exhibits lineaments on aerial photographs and lidar; locally contains thin discontinuous andesitic lava flows too small to map separately; weathers to rounded hills with deep regolith and poor exposure; commonly covered with lag of volcanic boulders; contains locally common "jigsaw" clasts in matrix-supported volcanic mudflows indicating brittle failure under high confining pressure (Pierson et al., 2018) typical of sector collapse volcanic landslides (Hacker et al., 2014; Biek et al., 2019); contains brecciated blocks of Paleozoic and Mesozoic strata large enough to be mapped at scale as chaotic blocks (Mount, 1952; Bromfield and Crittenden, 1971; Woodfill, 1972; Biek, 2022b) with five individual chaos blocks mapped as separate units (Tkc[n,p,p-w]); as discussed by Biek (2022a, 2022b), blocks of the Coyote Canyon chaos may have been emplaced as part of a debris-avalanche deposit that traveled as a semi-coherent block; smaller clasts composed of Paleozoic and Mesozoic strata increase in abundance within Tkc in proximity to mapped chaotic blocks; unit deposited as lahars, debris avalanches, and lava flows on distal flanks of stratovolcanoes above eastern Wasatch igneous belt (Bromfield, 1968; Woodfill, 1972; John, 1989b; Bryant, 1992; Leveinen, 1994; Hanson, 1995; Feher et al., 1996; Feher, 1997; Smyk et al., 2018); locally reworked by alluvial processes with alluvial and mudflow units exhibiting graded bedding; lower contact with Nugget Sandstone is an angular unconformity; as much as 1500 feet (460 m) thick northeast of Heber Valley.

Tkc(n) **Coyote Canyon chaos, Nugget Sandstone** (Early Oligocene to Late Eocene) – Two moderately brecciated blocks inferred to be sourced from the Jurassic Nugget Sandstone within the Coyote Canyon mudflow breccia (Tkc); one block is located approximately 1.5 miles (2.4 km) southwest of Webb Hollow and is primarily composed of brecciated cross-bedded sandstone, two large boulders of moderately deformed sandstone up to 60 feet (20 m) in diameter are present with discernible, randomly oriented bedding, exposure area of this block is approximately 2.7 acres (11,000 m^2); the second block is located just south of the Big Pole Canyon trailhead and is composed of heavily fractured sandstone and breccia, exposure area of this block is approximately 1 acre (4,000 m^2); within the surrounding mudflow breccia (Tkc), the percentage of sedimentary clasts relative to volcanic clasts increases with proximity to both chaos blocks; poor exposure precludes kinematic data to clarify emplacement mechanisms or source; as discussed by Biek (2022a), blocks of the Coyote Canyon chaos may have been emplaced as part of a debris-avalanche deposit that traveled as a semi-coherent slab; thickness unknown.

Tkc(p) **Coyote Canyon chaos, Park City Formation** (Early Oligocene to Late Eocene) – A single block composed of poorly exposed moderately brecciated fragments of sandstone and limestone inferred to be sourced primarily from the Park City Formation, as interpreted by Woodfill (1972); located approximately 1.5 miles (2.4 km) south of Webb Hollow; within the surrounding mudflow breccia (Tkc), the percentage of sedimentary clasts relative to volcanic clasts increases with proximity to the chaos block; poor exposure precludes kinematic data to clarify emplacement mechanisms or source; as discussed by Biek (2022a, 2022b), blocks of the Silver Creek chaos may have been emplaced as part of a debris-avalanche deposit that traveled as a semi-coherent slab; exposure area of this block is approximately 8 acres (33,000 m^2); thickness unknown.

Tkc(p-w)

Coyote Canyon chaos, Park City Formation and Weber Sandstone (Early Oligocene to Late Eocene) – A very large single block composed of moderately to heavily brecciated fragments of sandstone and limestone inferred to be sourced primarily from the Park City Formation and Weber Sandstone; Woodfill (1972) interpreted this exposure to be sourced from the Park City Formation, but large expsoures of thick-bedded and well-cemented sandstone reminiscent of the Weber Sandstone are present throughout the exposure; located approximately 2 miles (3.2 km) east of McDonalds Little Valley; within the surrounding mudflow breccia (Tkc), the percentage of sedimentary clasts relative to volcanic clasts increases with proximity to the chaos block; a few large, intact boulders of up to 30 feet (10 m) in diameter are present with discernible, randomly oriented bedding; poor exposure precludes kinematic data to clarify emplacement mechanisms or source; as discussed by Biek (2022a), blocks of the Coyote Canyon chaos may have been emplaced as part of a debris-avalanche deposit that traveled as a semi-coherent slab; exposure area of this large block is approximately 170 acres (688,000 m^2), partly covered by Quaternary deposits; thickness unknown.

Tks **Volcanic mudflow breccia of Silver Creek** (Early Oligocene to Late Eocene) – Andesitic volcanic mudflow breccia similar and likely equivalent to that of the volcanic breccia of Coyote canyon (Tkc); mapped north of the Provo River; light-gray andesitic to rhyodacitic volcanic mudflow deposits, minor ash-flow tuff, and minor lava flows; clasts are andesite and rhyodacite by field classification but chemically range from latite and trachyte to andesite and dacite (Bromfield et al., 1977); clasts are commonly as much as 5 to 10 feet (1.5–3 m) in diameter, consisting of highly brecciated, weathered, and unidentifiable igneous and local sedimentary rock fragments; volcaniclastic rocks are typically heterolithic but in places are monolithic (Biek, 2022b); best exposures occur in cliffs north of the Provo River; exhibits lineaments on aerial photographs and lidar; locally contains thin discontinuous andesitic lava flows too small to map separately; weathers to rounded hills with deep regolith and poor exposure; commonly covered with lag of volcanic boulders; contains locally common "jigsaw" clasts in matrix-supported volcanic mudflows indicating brittle failure under high confining pressure (Pierson et al., 2018) typical of sector collapse volcanic landslides (Hacker et al., 2014; Biek et al., 2019); contains brecciated blocks of Mesozoic strata large enough to be mapped at scale as chaotic blocks (Mount, 1952; Bromfield and Crittenden, 1971; Woodfill, 1972; Biek, 2022b) with two individual chaos blocks mapped as separate units (Tks[a,t]); as discussed by Biek (2022a, 2022b), blocks of the Silver Creek chaos may have been emplaced as part of a debris-avalanche deposit that traveled as a semi-coherent block; smaller clasts composed of Mesozoic strata increase in abundance within Tks in proximity to mapped chaotic blocks; unit deposited as lahars, debris avalanches, and lava flows on distal flanks of stratovolcanoes above eastern Wasatch igneous belt (Bromfield, 1968; Woodfill, 1972; John, 1989b; Bryant, 1992; Leveinen, 1994; Hanson, 1995; Feher et al., 1996; Feher, 1997; Smyk et al., 2018); locally reworked by alluvial processes with alluvial and mudflow units exhibiting graded bedding; locally contains petrified twigs and logs up to 3 feet (1 m) in diameter like those found near the Sunrise Rotary Regional Geologic Park (Milligan and Biek, 2019); lower contact is not observed in this quadrangle but is in angular discordance with underlying stratigraphy elsewhere; as much as 1500 feet (460 m) thick northeast of Heber Valley.

Tks(a) **Silver Creek chaos, Ankareh Formation, undivided** (Early Oligocene to Late Eocene) – A single large, poorly exposed, brecciated block composed of reddish-brown mudstone and siltstone, interpreted as Triassic Ankareh Formation (ŧa) within the surrounding Silver Creek mudflow breccia (Tks); identifiable by the presence of red, clay-rich soil and limited exposure of intact dark-red platy siltstone; located approximately 1.2 miles (1.9 km) north of the eastern margin of Jordanelle Reservoir; a few large, intact exposures up to 30 feet (10 m) in diameter are present with discernible, randomly oriented bedding; poor exposure precludes kinematic data to clarify emplacement mechanisms or source; as discussed by Biek (2022a), blocks of the Silver Creek chaos may have been emplaced as part of a debris-avalanche deposit that traveled as a semi-coherent slab; exposed area of this block is approximately 29 acres (117,000 m^2); thickness unknown.

Tks(t) **Silver Creek chaos, Thaynes Formation, undivided** (Early Oligocene to Late Eocene) – A single large block composed of moderately brecciated fragments of sandstone and limestone inferred to be sourced from the Thaynes Formation as interpreted by Woodfill (1972); located approximately 1.3 miles (2.1 km) north of the eastern margin of Jordanelle Reservoir; a few large, intact exposures up to 30 feet (10 m) in diameter are present with discernible, randomly oriented bedding; poor exposure precludes kinematic data to clarify emplacement mechanisms or source; as discussed by Biek (2022a), blocks of the Silver Creek chaos may have been emplaced as part of a debris-avalanche deposit that traveled as a semi-coherent slab; exposure area of this block is approximately 34 acres (138,000 m^2); thickness unknown.

Toc **Older conglomerate** (Eocene?) – Pebble- to boulder-conglomerate with subangular to rounded clasts sourced from dominantly Weber and Nugget Sandstones with inferred (from water well data, not exposed) interbedded sandstone and mudstone; poorly exposed and mapped only as small exposure along the northern margin of the quadrangle; upper contact with the Keetley Volcanics is poorly exposed but appears to be both locally disconformable (Biek, 2022a), conformable, and interfingering (Reeher, 2024); recent construction cuts in the neighboring Park City East quadrangle exposed interfingering relationships between this unit and Tks; Bryant (1990) reports an abundance of volcanic clasts within the unit in the Porcupine Ridge area 20 miles (32 km) north of the map area; thickness is not complete in quadrangle, inferred to be about 150 feet (45 m) thick.

unconformity

JURASSIC

Twin Creek Limestone (Middle Jurassic, Callovian to middle Bajocian) – The formation consists of six members, from youngest to oldest: Giraffe Creek, Leeds Creek, Watton Canyon, Boundary Ridge, Rich, and Sliderock. This usage follows Sprinkel et al. (2011), which treats the Gypsum Spring as a separate formation. Although the Sliderock, Rich, and Boundary Ridge Members are exposed in the southwestern corner of this map area, the three youngest members (Giraffe Creek, Leeds Creek, and Watton Canyon) are not present within the quadrangle or shown on the cross section. A Middle Jurassic age is assigned based on Imlay (1967, 1980), Sprinkel et al. (2011), and Doelling et al. (2013).

Jtb **Twin Creek Limestone, Boundary Ridge Member** (Middle Jurassic, Bathonian) – Interbedded reddish-brown to greenish-gray, thin-bedded to laminated mudstone, red to green to yellow siltstone, silty to fine-grained sandy limestone, and oolitic limestone; upper part is non-resistant, forms slopes, and weathers to poorly exposed saddles; basal limestone beds commonly form resistant ridges; incomplete thickness exposed in quadrangle; 145 feet (44 m) thick in the Center Creek quadrangle (Biek et al., 2003); map-based thickness of about 120 feet (25 m) near Heber City.

Jtr **Twin Creek Limestone, Rich Member** (Middle Jurassic, Bajocian) – Medium- to light-gray and light-brownish-gray, thin- to medium-bedded, finely crystalline limestone, argillaceous limestone, and calcareous sandstone with ripple laminations; forms small ledges and slopes; pencil cleavage is common; lower gradational contact typically corresponds to a break in slope between more resistant Jts and less resistant argillaceous Jtr; Imlay (1967) reports a thickness of 125 feet (40 m) near Peoa and Oakley; Sprinkel and Doelling report a thickness of 171 feet (52 m) near Peoa and Oakley (UGS unpublished data, June 22, 1999); in the southern Heber Valley area, Rich strata are about 160 feet (50 m) thick at the northwestern side of Deer Creek Reservoir (Biek and Lowe, 2009) and 116 feet (35 m) thick in the Center Creek quadrangle (Biek et al., 2003); map-based thickness is about 160 feet (50 m) near Heber City.

Jts **Twin Creek Limestone, Slide Rock Member** (Middle Jurassic, Bajocian) – Brownish-gray, thin- to medium-bedded, shaley limestone with a conchoidal fracture habit, finely crystalline limestone with crinoid columns and fossil hash, and micritic limestone that weathers to pencil-like fragments; weathers light-gray and forms ledges; lower contact corresponds to the J-2 unconformity and is sharp with a change from the gray, ledgy limestone of Jts to reddish-brown siltstone slopes of Jg; about 100 to 150 feet (30– 45 m) thick in the Park City West quadrangle (Biek et al., 2022); map-based thickness is about 150 feet (45 m) near Heber City.

J-2 *unconformity (Pipirngos and O'Sullivan, 1978)*

Jg **Gypsum Spring Formation** (Middle to Early Jurassic, late Pliensbachian to early Bajocian) – Dark-reddish-brown and locally yellowish-brown, fine- to medium-grained silty sandstone; forms slopes and saddles; Sprinkel and Doelling report a thin (1ft) basal chert-pebble sandstone near Peoa (UGS unpublished data, June 22, 1999); Imlay (1967) included Gypsum Spring as a member of the Twin Creek Limestone (Jt), usage here follows Sprinkel et al. (2011) where the Gypsum Spring is treated as a separate formation; lower contact is sharp and planar and corresponds to a prominent lithologic and topographic change, with resistant cross-bedded sandstone of J₮n below and non-resistant dark-reddish-brown silty sandstone of Jg above; Imlay (1967) reported that the unit is 22 feet (7 m) thick in outcrops near Peoa and Oakley, but thickens greatly to the northwest to about 140 feet (43 m) in Burr Fork near the top of Emigration Canyon and 208 feet (63 m) at Devils Slide; map-based thickness is about 35 feet (10 m) near Heber City.

J-1 *unconformity (Pipiringos and O'Sullivan, 1978)*

JURASSIC-TRIASSIC

J₮n **Nugget Sandstone** (Early Jurassic to Late Triassic) – Reddish-orange to pale-orange, fine- to medium-grained, well-sorted, moderately well cemented, quartz sandstone with well-rounded, frosted quartz grains; large-scale cross-stratification in the upper part with planar beds near the base; forms ridges and weathers to blocky outcrops; lower contact corresponds to the base of the resistant J₮n and the underlying non-resistant ₮a; correlative with the entire Glen

Canyon Group of the Colorado Plateau (Wingate Sandstone/Moenave Formation, Kayenta Formation, and Navajo Sandstone) (Sprinkel et al., 2011); Sprinkel et al. (2011) summarized age control, primarily aetosaur and dinosaur tracks, indicating the Triassic-Jurassic boundary is within the lower part; based on this the J-0 unconformity of Pipiringos and O'Sullivan (1978) probably does not exist in northern Utah; lower contact with Triassic Ankerah Formation (Ŧa) is obscured by Paleogene volcanic rocks and not exposed in the quadrangle; map-based thickness of about 900 to 1200 feet (275–365 m) thick along the southwestern margin of Heber Valley.

TRIASSIC

Ŧa **Ankareh Formation, undivided** (Late and Early Triassic) – Not exposed, shown in cross section only; regionally consists of three members—the upper Gartra Grit and Mahogany members— with a major regional unconformity, the Ŧ3 unconformity of Pipiringos and O'Sullivan (1978), separating the middle Gartra Grit and lower Mahogany members (Kummel, 1954); 1485 feet (453 m) thick southwest of Heber Valley (Baker, 1964); inferred to be about 1400 feet (425 m) thick as portrayed on cross section.

Ŧt **Thaynes Formation** (Early Triassic) – Not exposed, shown in cross section only; in Park City area to the east, Thaynes strata are divisible into three members: an upper carbonate member, a middle clastic member, and a lower carbonate member; combined thickness of about 1000 feet (300 m) in the Park City West quadrangle (Biek et al., 2022) as portrayed on cross section.

Ŧw **Woodside Shale** (Early Triassic) – Not exposed, shown in cross section only; Pipiringos and O'Sullivan (1978) suggest the Ŧ-1 unconformity is present between Triassic and Permian rocks in northern Utah, however this contact has been reported as conformable by Boutwell (1912) and Cheney (1957) and recent work by Saltzman and Sedlacek (2013), Davydov et al. (2018), and Burger et al. (2019) suggests continuous deposition across this boundary; Baker (1964) reported a thickness of 315 feet (95 m) southwest of Heber Valley; Biek et al., (2022) reported a thickness of about 500 feet (150 m) north of Silver Fork and Brighton in Big Cottonwood Canyon; thickness is assumed to be about 330 feet (100 m) as portrayed on cross section.

Ŧ-1 unconformity (Pipringos and O'Sullivan, 1978)

PERMIAN

Pp **Park City and Phosphoria Formations, undivided** (Middle to Early Permian) – Not exposed, shown in cross section only; Burger et al. (2019) summarized fossil-based age control for the Park City and Phosphoria Formations in northern Utah and southern Idaho; Davydov et al. (2018) reported a U–Pb CA-IDTIMS zircon age of 260.57 ± 0.007 Ma from an ash bed in the upper part of the unit in southeast Idaho; map patterns suggest a thickness of about 700 feet (210 m) at Boutwell's (1912) type section in Big Cottonwood Canyon (Biek et al., 2022) as portrayed on cross section.

PERMIAN-PENNSYLVANIAN

PPw **Weber Sandstone** (Early Permian? to Middle Pennsylvanian) – Very pale yellowish-gray and grayish-orange to white, fine-grained, indurated, thick-bedded, dominantly quartz arenite and locally calcareous sandstone; contains a few thin, light-gray limestone, cherty limestone, and dolomite interbeds; commonly highly fractured; resistant and forms ridges; Middle Pennsylvanian and Early Permian age is based on fusulinids from Bissell and Childs (1958) and Bissell (1964); Coogan and King (2016) report a thickness of 2600 feet (790 m) near Morgan; Bryant (1990) reports a thickness of 985–1640 feet (300–500 m) in the Wasatch Range; map based thickness of approximately 1400 feet (425 m).

PENNSYLVANIAN-DEVONIAN

PDu **Pennsylvanian through Devonian rocks, undivided** (Middle Pennsylvanian to Late Devonian) – Not exposed, shown on cross section only; along the southern flank of the Uinta mountains to the east of the Francis quadrangle, this section includes the Middle Pennsylvanian Morgan Formation, the Early Pennsylvanian Round Valley Limestone, the Late Mississippian Doughnut and Humbug Formations, the Mississippian Madison Limestone, and undifferentiated upper Devonian rocks (Bryant, 1990); in Heber Valley to the east of the Francis quadrangle, this section includes the Early Pennsylvanian Round Valley Limestone, the Late Mississippian Doughnut and Humbug Formations, and the Mississippian Deseret and Gardison Limestones (Biek, 2022b); combined estimated thickness of approximately 2600 feet (800 m) in western Uinta Mountains (Bryant, 1990) as portrayed on cross section.

unconformity

CAMBRIAN-NEOPROTEROZOIC

ЄZu **Cambrian through Neoproterozoic rocks, undifferentiated** (Cambrian to Neoproterozoic) – Not exposed, shown on cross section only; to the east of the Francis quadrangle, units outcrop along the southern flank of the Uinta Mountains represented by the Neoproterozoic Uinta Mountain group and does not include Cambrian rocks (Bryant, 1990); to the west of the Francis quadrangle, this unit also includes the Cambrian Ophir Formation, the Cambrian Tintic Quartzite, the Neoproterozoic Mineral Fork Formation, and the Neoproterozoic Big Cottonwood Formation (Biek, 2022b); presumably the Cambrian section pinches out beneath the quadrangle against the Uinta arch, but merged unit does not portray this pinch out on cross section; thickness of at least 12,000 feet (3650 m) in western Uinta Mountains (Bryant, 1990).

ACKNOWLEDGMENTS

This geologic map was funded by the Utah Geological Survey (UGS) and the U.S. Geological Survey (USGS), National Cooperative Geologic Mapping Program through USGS STATEMAP award number G22AC00466 (2023–2025). UGS staff Matthew Morriss, Emily Kleber, Zach Anderson, Adam McKean, Stefan Kirby, Don Clark, as well as Mike Stearns of Utah Valley University, provided helpful and engaging discussions about the geology both in the field and in the office. We thank Jordanelle State Park and Victory Ranch for facilitating access to their properties. UGS staff Matthew Morriss, Stefan Kirby, Stephanie Carney, and Darlene Batatian improved this map and text through their thoughtful reviews.

REFERENCES

Allmendinger, R.W., 1992, Fold and thrust tectonics of the western United States exclusive of the accreted terranes, *in* Burchfiel, B.C., Lipman, P.W., and Zoback, M.L., editors., The Cordilleran Orogen—Conterminous U.S., volume G-3: Boulder, Colorado, Geological Society of America, p. 583–607, https://doi.org/10.1130/DNAG-GNA-G3.583.

Anderson, G., 1915, Stream piracy of the Provo and Weber rivers, Utah: American Journal of Science, v. 4, no. 237, p. 314–316.

Ashland, F.X., 2003, The feasibility of collecting accurate landslide-loss data in Utah: Utah Geological Survey Open-File Report 410, 25 p., https://doi.org/10.34191/OFR-410.

Baker, A.A., 1964, Geology of the Aspen Grove quadrangle, Utah: U.S. Geological Survey Geologic Quadrangle Map GQ-239, 9 p., 1 plate, scale 1:24,000.

Baker, C.H., Jr., and Peterson, D.L., 1970, Water resources of the Heber-Kamas-Park City area north-central Utah, with a section on a gravity and aeromagnetic survey of Heber and Rhodes Valleys: Utah Department of Natural Resources, Division of Water Rights Technical Publication 27, 91 p.

Biek, R.F., 2022a, Geologic map of the Park City East quadrangle, Summit and Wasatch Counties, Utah: Utah Geological Survey Map M-296DM, scale 1:24,000, https://doi.org/10.34191/M-296DM.

Biek, R.F., 2022b, Geologic map of the Heber City quadrangle, Wasatch and Summit Counties, Utah: Utah Geological Survey Map M-295DM, scale 1:24,000, https://doi.org/10.34191/M-295DM.

Biek, R.F., Hylland, M.D., Welsh, J.E., and Lowe, M., 2003, Geologic map of the Center Creek quadrangle, Wasatch County, Utah: Utah Geological Survey Map M-192, scale 1:24,000, https://doi.org/10.34191/M-192.

Biek, R.F., and Lowe, M., 2009, Geologic map of the Charleston quadrangle, Wasatch County, Utah: Utah Geological Survey Map 236, 2 plates, scale 1:24,000, https://doi.org/10.34191/M-236.

Biek, R.F., Rowley, P.D., and Hacker, D.B., 2019, The gigantic Markagunt and Sevier gravity slides resulting from mid-Cenozoic catastrophic mega-scale failure of the Marysvale volcanic field, Utah, USA: Geological Society of America Field Guide 56, 121 p.

Biek, R.F., Yonkee, W.A., and Loughlin, W.D., 2022, Geologic map of the Park City West quadrangle, Summit and Salt Lake Counties, Utah: Utah Geological Survey Map 297DM, 21 p., 2 plates, scale 1:24,000, https://doi.org/10.34191/M-297DM.

Bird, P., 1984, Laramide crustal thickening event in the Rocky Mountain foreland and Great Plains: Tectonics, v. 3, no. 7, p. 741–758, https://doi.org/10.1029/TC003i007p00741.

Bissell, H.J., 1964, Lithology and petrography of the Weber Formation, in Utah and Colorado, *in* Sabatka, E.F., editor, Guidebook to the geology and mineral resources of the Uinta Basin—Utah's hydrocarbon storehouse: Thirteenth Annual Field Conference, Utah Geological Association, p. 67–91.

Bissell, H.J., and Childs, O.E., 1958, The Weber Formation of Utah and Colorado, *in* Symposium on Pennsylvanian rocks of Colorado and adjacent areas: Denver, Colorado, Rocky Mountain Association of Geologists, p. 26–30.

Black, B.D., and Hecker, S., 1999, Fault number 2391, East Kamas fault, *in* Quaternary fault and fold database of the United States: U.S. Geological Survey, https://earthquakes.usgs.gov/hazards/qfaults, accessed 02/19/2024 02:04 PM.

Blakey, R.C., 1994, Paleogeographic and tectonic controls on some Lower and Middle Jurassic erg deposits, Colorado Plateau, *in* Caputo, M.V., Peterson, J.A., and Franczyk, K.J., editors, Mesozoic systems of the Rocky Mountain Region: Rocky Mountain Section of the Society for Sedimentary Geology (SEPM), p. 273–279.

Boutwell, J.M., 1912, Geology and ore deposits of the Park City district, with contributions by L.H. Woosley: United States Geological Survey Professional Paper 77, 231 p.

Bradley, M.D., 1988, Structural evolution of the Uinta Mountains, Utah, and their interaction with the Utah-Wyoming salient of the Sevier overthrust belt: Salt Lake City, The University of Utah, Ph.D. dissertation, 178 p.

Bradley, M.D., 1995, Timing of the Laramide rise of the Uinta Mountains, Utah and Colorado, *in* Jones, R., editor, Resources of southwest Wyoming: 1995 Field Conference Guidebook, Wyoming Geological Association, p. 31–44.

Bradley, M.D., and Bruhn, R.L., 1988, Structural interactions between the Uinta arch and the overthrust belt, north-central Utah—Implications of strain trajectories and displacement modeling, *in* Schmidt, C.J., and Perry, W.J., Jr., editors, Interaction of the Rocky Mountain foreland and the Cordilleran thrust belt, volume 171: Geological Society of America, p. 431–446, https://doi.org/10.1130/MEM171-p431.

Bromfield, C.S., 1968, Source of Keetley volcanic field: United States Geological Survey Professional Paper 600-A, 33 p.

Bromfield, C.S., and Crittenden, M.D., 1971, Geologic map of the Park City East quadrangle, Summit and Wasatch Counties, Utah: United States Geological Survey Map GQ-852, scale 1:24,000, https://doi.org/10.3133/gq852.

Bromfield, C.S., Erickson, A.J., Haddadin, M.A., and Mehnert, H.H., 1977, Potassium-argon ages of intrusion, extrusion, and associated ore deposits, Park City mining district, Utah: Economic Geology, v. 72, no. 5, p. 837–848, http://doi.org/10.2113/gsecongeo.72.5.837.

Bruhn, R.L., Picard, M.D., and Isby, J.S., 1986, Tectonics and sedimentology of Uinta Arch, western Uinta Mountains, and Uinta Basin, *in* Peterson, J. A., editor, Paleotectonics and sedimentation in the Rocky Mountain Region, United States, volume 32: Association of Petroleum Geologists Memoir, p. 333–352.

Bryant, B., 1990, Geologic map of the Salt Lake City 30′ X 60′ quadrangle: Utah Geological Survey Map M-190DM, scale 1:100,000, https://doi.org/10.34191/M-190dm.

Bryant, B., 1992, Geologic and structure maps of the Salt Lake City 1° x 2° quadrangle, Utah and Wyoming: U.S. Geological Survey Miscellaneous Investigations Series Map I-1997, scale 1:125,000.

Bryant, B., and Nichols, D.J., 1988, Late Mesozoic and early Tertiary reactivation of an ancient crustal boundary along the Uinta trend and its interaction with the Sevier orogenic belt, *in* Schmidt, C.J., and Perry, W.J., Jr., editors, Interaction of the Rocky Mountain foreland and the Cordilleran thrust belt, volume 171: Geological Society of America, p. 411–430, https://doi.org/10.1130/MEM171-p411.

Burger, B.J., Vargas Estrada, M., and Gustin, M.S., 2019, What caused Earth's largest mass extinction event? New evidence from the Permian-Triassic boundary in northeastern Utah: Global and Planetary Change, v. 177, p. 81–100, https://doi.org/10.1016/j.gloplacha.2019.03.013.

Cheney, T.M., 1957, Phosphate in Utah: Utah Geological and Mineralogical Survey Bulletin, v. 59, 54 p., https://doi.org/10.34191/B-59.

Clark, D.L., 2020, The Uinta-Tooele structural zone–what's in a name?: Utah Geological Survey, Survey Notes, v. 52, no. 2, p. 4–5., https://doi.org/10.34191/SNT-52-2.

Clark, D.L., Oviatt, C.G., and Dinter, D.A., 2020, Geologic map of the Tooele 30′ x 60′ quadrangle, Tooele, Salt Lake, and Davis Counties, Utah: Utah Geological Survey Map M-284DM, scale 1:62,000, https://doi.org/10.34191/M-284DM.

Connors, C.D., Roberts, H., Maloy, J., Ogden, J., and Comisac, P., 2023, findSD—An application for determination of bedding-plane attitudes from high-resolution digital elevation models [abs.]: Geological Society of America Annual Conference, Pittsburgh, Pennsylvania.

Constenius, K.N., 1996, Late Paleogene extensional collapse of the Cordilleran foreland fold and thrust belt: Geological Society of America Bulletin, v. 108, no. 1, p. 20–39, https://doi.org/10.1130/0016-7606(1996)108<0020:LPECOT>2.3.CO;2.

Constenius, K.N., Clark, D.L., King, J.K., and Ehler, J.B., 2011, Interim geologic map of the Provo 30' x 60' quadrangle, Salt Lake, Utah, and Wasatch Counties, Utah: Utah Geological Survey Open-File Report 586DM, 42 p., 1 plate, scale 1:62,500, https://doi.org/10.34191/OFR-586DM.

Coogan, J.C., and King, J.K., 2016, Interim geologic map of the Ogden 30' x 60' quadrangle, Box Elder, Cache, Davis, Morgan, Rich, and Summit Counties, Utah, and Uinta County, Wyoming: Utah Geological Survey Map OFR-653DM, scale 1:62,000, https://doi.org/10.34191/OFR-653dm.

Crittenden, M.D.J., 1976, Stratigraphic and structural setting of the Cottonwood area, Utah, *in* Hill, J.G., editor, Symposium of the Cordilleran hingeline: Rocky Mountain Association of Geologists, p. 363–379.

Davydov, V.I., Biakov, A.S., Schmitz, M.D., and Silantiev, V.V., 2018, Radioisotopic calibration of the Guadalupian (middle Permian) series—Review and updates: Earth-Science Reviews, v. 176, p. 222–240, https://doi.org/10.1016/j.earscirev.2017.10.011.

DeCelles, P.G., 1994, Late Cretaceous-Paleocene synorogenic sedimentation and kinematic history of the Sevier thrust belt, northeast Utah and southwest Wyoming: Geological Society of America Bulletin, v. 106, no. 1, p. 32–56, https://doi.org/10.1130/0016-7606(1994)106<0032:LCPSSA>2.3.CO;2.

Dickinson, W.R., Klute, M.A., Hayes, M.J., Janecke, S.U., Lundin, E.R., McKittrick, M.A., and Olivares, M.D., 1988, Paleogeographic and paleotectonic setting of Laramide sedimentary basins in the central Rocky Mountain region: Geological Society of America Bulletin, v. 100, no. 7, p. 1023–1039, https://doi.org/10.1130/0016-7606(1988)100<1023:Papsol>2.3.Co;2.

Dickinson, W.R., and Snyder, W.S., 1978, Plate tectonics of the Laramide orogeny, *in* Matthews, V., editor, Laramide folding associated with basement block faulting in the western United States, volume 151: Geolgical Society of America Memior, p. 355–366, https://doi.org/10.1130/MEM151-p355.

Doelling, H., Sprinkel, D., Kowallis, B., and Kuehne, P., 2013, Temple Cap and Carmel Formations in the Henry Mountains basin, Wayne and Garfield Counties, Utah, *in* Morris, T.H., and Ressetar, R., editors, The San Rafael Swell and Henry Mountains basin—geologic centerpeice of Utah: Utah Geological Association Publication 42, p. 279–318.

Eardley, A.J., and Hatch, R.A., 1940, Proterozoic (?) rocks in Utah: Geological Society of America Bulletin, v. 51, no. 6, p. 795–843, https://doi.org/10.1130/gsab-51-795.

Fenneman, N.M., and Johnson, D.W., 1946, Physiographic divisions of the conterminous U.S.: U.S. Geological Survey data release, https://doi.org/10.5066/P9B1S3K8.

Feher, L.A., 1997, Petrogenesis of the Keetley Volcanics in Summit and Wasatch Counties, north-central Utah: East Lansing, Michigan State University, M.S. thesis, 95 p.

Feher, L.A., Constenius, K.N., and Vogel, T.A., 1996, Relationships between the Wasatch intrusive belt and the Keetley Volcanics, north-central Utah [abs.]: Geological Society of America Abstracts with Programs, v. 28, no. 7, p. 483.

Forrester, D.J., 1937, Structure of the Uinta Mountains: Geological Society of America Bulletin, v. 48, no. 5, p. 631–666, https://doi.org/10.1130/gsab-48-631.

Hacker, D.B., Biek, R.F., and Rowley, P.D., 2014, Catastrophic emplacement of the gigantic Markagunt gravity slide, southwest Utah—implications for hazards associated with sector collapse of volcanic fields: Geology, v. 42, no. 11, 4 p., https://doi.org/10.1130/G35896.1.

Hanson, S.L., 1995, Mineralogy, petrology, geochemistry and crystal size distribution of Tertiary plutons of the central Wasatch Mountains, Utah: Salt Lake City, The University of Utah, Ph.D. dissertation, 371 p.

Hintze, L.F., 1988, Geologic history of Utah: Brigham Young University Geology Studies Special Publication 7, 202 p.

Houston, R.S., Erslev, E.A., Frost, C.D., Karlstrom, K.E., Page, N.J., Zientek, M.L., Reed, J.C., Jr., Snyder, G.L., Worl, R.G., Bryant, B., Reynolds, M.W., and Peterman, Z.E., 1993, The Wyoming province, *in* Reed, J.C., Jr., Bickford, M.E., Houston, R.S., Link, P.K., Rankin, D.W., Sims, P.K., and Schmus, W.R.V., editors, Precambrian—Conterminous U.S., volume C-2: Geological Society of America, p. 121–170, https://doi.org/10.1130/DNAG-GNA-C2.121.

Hurlow, H.A., 2002, The geology of the Kamas-Coalville region, Summit County, Utah, and its relation to ground-water conditions: Utah Geological Survey WRB-29, 70 p., https://doi.org/10.34191/WRB-29.

Imlay, R.W., 1967, Twin Creek limestone (Jurassic) in the western interior of the United States 540, p. 105, https://doi.org/10.3133/pp540.

Imlay, R.W., 1980, Jurassic paleobiogeography of the conterminous United States in its continental setting: United States Geological Survey Professional Paper 1062, 134 p., https://doi.org/10.3133/pp1062.

Jensen, C.G., Christiansen, E.H., and Keith, J.D., 2022, Multi-stage construction of the Little Cottonwood stock, Utah, USA—Origin, intrusion, venting, mineralization, and mass movement: Geosphere, v. 18, no. 4, p. 1264–1296, https://doi.org/10.1130/ges02369.1.

John, D.A., 1987, Evolution of hydrothermal fluids in intrusions of the central Wasatch Mountains, Utah: Palo Alto, California, Stanford University, Ph.D. dissertation, 236 p.

John, D.A., 1989a, Evolution of hydrothermal fluids in the Park Premier Stock, central Wasatch Mountains, Utah: Economic Geology, v. 84, no. 4, p. 879–902, https://doi.org/10.2113/gsecongeo.84.4.879.

John, D.A., 1989b, Geologic setting, depths of emplacement, and regional distribution of fluid inclusions in intrusions of the central Wasatch Mountains, Utah: Economic Geology, v. 84, no. 2, p. 386–409, https://doi.org/10.2113/gsecongeo.84.2.386.

Kocurek, G., and Dott, R.H.J., 1983, Jurassic paleogeography and paleoclimate of the central and southern Rocky Mountains region, *in* Reynolds, M.W., and Dolly, E.D., editors, Mesozoic paleogeography of the west-central United States, Volume 2: Rocky Mountain Society of Economic Paleontologists and Mineralogists, p. 101–116.

Kummel, B., 1954, Triassic stratigraphy of southeastern Idaho and adjacent areas: United States Geological Survey Professional Paper 254-H, p. 165–194, https://doi.org/10.3133/pp254H.

Lamerson, P.R., 1982, The Fossil Basin and its relationship to the Absaroka thrust system, Wyoming and Utah, *in* Powers, R.B., editor, Geologic studies of the Cordilleran thrust belt, Volume 1: Rocky Mountain Association of Geologists, p. 279–340.

Leveinen, J.E., 1994, Petrology of the Keetley Volcanics in Summit and Wasatch Counties, north-central Utah: Duluth, University of Minnesota, M.S. thesis, 175 p.

Milligan, M., and Biek, R.F., 2019, Park City Sunrise Rotary Regional Geologic Park, Summit County, Utah: Utah Geological Survey, Survey Notes 51, p. 12–13, https://doi.org/10.34191/SNT-51-3.

Mount, D.L., 1952, Geology of the Wanship-Park City region, Utah: Salt Lake City, University of Utah, M.S. thesis, 35 p., 1 plate, scale 1:31,680.

Munroe, J.S., and Laabs, B.J.C., 2009, Glacial geologic map of the Uinta Mountains area, Utah and Wyoming: Utah Geological Survey Map MP-09-4DM, scale 1:100,000, https://doi.org/10.34191/MP-09-4dm.

Munroe, J.S., and Laabs, B.J.C., 2017, Combining radiocarbon and cosmogenic ages to constrain the timing of the last glacial-interglacial transition in the Uinta Mountains, Utah, USA: Geology, v. 45, no. 2, p. 171–174, https://doi.org/10.1130/G38156.1.

O'Toole, W.L., 1951, Geology of the Keetley-Kamas volcanic area: Salt Lake City, University of Utah, M.S. thesis, 38 p.

Peters, S.E., and Gaines, R.R., 2012, Formation of the 'Great Unconformity' as a trigger for the Cambrian explosion: Nature, v. 484, no. 7394, p. 363–366, https://doi.org/10.1038/nature10969.

Peterson, F., 1994, Sand dunes, sabkhas, streams, and shallow seas—Jurassic paleogeography in the southern part of the Western Interior Basin, *in* Caputo, M.V., Peterson, J.A., and Franczyk, K.J., editors, Mesozoic systems of the Rocky Mountain Region: Rocky Mountain Section of the Society for Sedimentary Gelogy (SEPM), p. 233–272.

Picha, F., and Gibson, R.I., 1985, Cordilleran hingeline—Late Precambrian rifted margin of the North American craton and its impact on the depositional and structural history, Utah and Nevada: Geology, v. 13, no. 7, p. 465–468, http://doi.org/10.1130/0091-7613(1985)13<465:Chlprm>2.0.Co;2.

Pierce, K.L., Licciardi, J.M., Good, J.M., and Jaworowski, C., 2018, Pleistocene glaciation of the Jackson Hole area, Wyoming: United States Geological Survey Professional Paper 1835, 55 p., https://doi.org/10.3133/pp1835.

Pierson, T.C., Siebert, L., Harpel, C.J., and Scott, K.M., 2018, Geologic field-trip guide of volcaniclastic sediments from snow- and ice-capped volcanoes—Mount St. Helens, Washington, and Mount Hood, Oregon: U.S. Geological Survey Scientific Investigations Report 2017–5022–F, 97 p., https://doi.org/10.3133/sir20175022F.

Pipiringos, G.N., and O'Sullivan, R.B., 1978, Principal unconformities in Triassic and Jurassic rocks, western interior United States—A preliminary survey: United States Geological Survey Professional Paper 1035A, 29 p., http://doi.org/10.3133/pp1035A.

Quirk, B.J., Moore, J.R., Laabs, B.J.C., Plummer, M.A., and Caffee, M.W., 2020, Latest Pleistocene glacial and climate history of the Wasatch Range, Utah: Quaternary Science Reviews, v. 238, p. 1–17, https://doi.org/10.1016/j.quascirev.2020.106313.

Reeher, L.J., 2024, Interim geologic map of the Kamas quadrangle, Summit and Wasatch Counties, Utah: Utah Geological Survey Open-File Report 763, 16 p., 2 plates, scale 1:24,000, https://doi.org/10.34191/OFR-763.

Royse, F.J., 1993, An overview of the geologic structure of the thrust belt in Wyoming, northern Utah, and eastern Idaho, *in* Snoke, A.W., Steidtmann, J.R., and Roberts, S.M., editors, Geology of Wyoming, volume 5: Geological Survey of Wyoming Memoir, p. 272–311.

Royse, F.J., Warner, M.A., and Reese, D.L., 1975, Thrust belt sturctural geometry and related stratigraphic problems Wyoming-Idaho-northern Utah, *in* Bolyard, D.W., editor, Symposium of deep drilling frontiers in the Central Rocky Mountains: Rocky Mountain Association of Geologists, p. 41–54.

Saltzman, M.R., and Sedlacek, A.R.C., 2013, Chemostratigraphy indicates a relatively complete Late Permian to Early Triassic sequence in the western United States: Geology, v. 41, no. 4, p. 399–402, https://doi.org/10.1130/G33906.1.

Smyk, E., Hollings, P., Baker, M., Cooke, D.R., Thompson, J.A., Thompson, J.M., and Creaser, R., 2018, Geochemistry and geochronology of the intrusive rocks of the central Wasatch Mountains igneous belt, Utah, USA—implications for porphyry mineralization, *in* Emerman, S.H., Schamel, S., and Simmons, S., editors, Geofluids of Utah: Utah Geological Association Publication 47, p. 305–327.

Sprinkel, D., Doelling, H., Kowallis, B., Waanders, G., and Kuehne, P., 2011, Early results of a study of Middle Jurassic strata in the Sevier fold and thrust belt, Utah, *in* Sprinkel, D., Yonkee, A., and Chidsey, T.C., editors, Seveir thrust belt-northern and central utah and adjacent areas: Utah Geological Association Publication 40, p. 151–172.

Stearns, M.A., Bartley, J.M., Bowman, J.R., Forster, C.W., Beno, C.J., Riddle, D.D., Callis, S.J., and Udy, N.D., 2020, Simultaneous magmatic and hydrothermal regimes in Alta–Little Cottonwood stocks, Utah, USA, recorded using multiphase U-Pb petrochronology: Geosciences, v. 10, no. 4, p. 129–150, https://doi.org/10.3390/geosciences10040129.

Sullivan, J.T., Nelson, A.R., LaForge, R.C., Wood, C.K., and Hansen, R.A., 1988, Central Utah regional seismotectonic study for U.S. Bureau of Reclamation dams in the Wasatch Mountains: U.S. Bureau of Reclamation Seismotectonic Report 88-5, 269 p.

Thomas, H.D., and Krueger, M.L., 1946, Late Paleozoic and Early Mesozoic stratigraphy of Uinta Mountains, Utah: Association of American Petroleum Geologists Bulletin, v. 30, no. 8, p. 1255–1293, https://doi.org/10.1306/3d93385c-16b1-11d7-8645000102c1865d.

USDA National Agriculture Imagery Program (NAIP), 2009, Digital aerial stereo-photography, image size12 microns or 2117 pixels per inch, 3-band natural color, scale 1:40,000.

Utah Geospatial Resource Center (UGRC), State Geographic Information Database, 2020, 0.5-meter northern and central Utah lidar elevation data: Online, https://gis.utah.gov/data/elevation-and-terrain/2020-lidar-northern-central-utah/.

Vogel, T.A., Cambray, F.W., and Constenius, K.N., 2001, Origin and emplacement of igneous rocks in the central Wasatch Mountains, Utah: Rocky Mountain Geology, v. 36, no. 2, p. 119–162, https://doi.org/10.2113/gsrocky.36.2.119.

Vogel, T.A., Cambray, F.W., Feher, L., Constenius, K.N., John, D.A., and Ballantyne, G.H., 1998, Petrochemistry and emplacement history of the Wasatch igneous belt, *in* John, D.A., Ballantyne, G.H., and Thompson, T.B., editors, Geology and ore deposits of the Oquirrh and Wasatch Mountains, Utah: Society of Economic Geologists Guidebook Series Volume 29, p. 35–46, https://doi.org/10.5382/gb.29.

Weil, A.B., and Yonkee, A., 2023, The Laramide orogeny—Current understanding of the structural style, timing, and spatial distribution of the classic foreland thick-skinned tectonic system, *in* Whitmeyer, S. J., Williams, M.L., Kellett, D.A., and Tikoff, B., editors, Laurentia—Turning points in the cvolution of a continent: Geological Society of America Memoir 220, p. 707–771, https://doi.org/10.1130/2022.1220(33).

Woodfill, R.D., 1972, A geologic and petrographic investigation of a northern part of the Keetley volcanic field, Summit and Wasatch Counties, Utah: West Lafayette, Indiana, Purdue University, Ph.D. dissertation, 168 p.

Yonkee, W.A., Dehler, C.D., Link, P.K., Balgord, E.A., Keeley, J.A., Hayes, D.S., Wells, M.L., Fanning, C.M., and Johnston, S.M., 2014, Tectono-stratigraphic framework of Neoproterozoic to Cambrian strata, west-central U.S.—Protracted rifting, glaciation, and evolution of the North American Cordilleran margin: Earth-Science Reviews, v. 136, p. 59–95, https://doi.org/10.1016/j.earscirev.2014.05.004.

Yonkee, W.A., and Weil, A.B., 2015, Tectonic evolution of the Sevier and Laramide belts within the North American Cordillera orogenic system: Earth-Science Reviews, v. 150, p. 531–593, https://doi.org/10.1016/j.earscirev.2015.08.001.

Zoback, M.L., 1983, Structure and Cenozoic tectonism along the Wasatch fault zone, Utah, *in* Miller, D.M., Todd, V.R., and Howard, K.A., editors, Tectonic and stratigraphic studies in the eastern Great Basin:, Geological Society of America Memior 157, p. 3–27, https://doi.org/10.1130/MEM157-p3.